Frequency stability of an islanded grid supplied by hydropower plants

M. Cadeddu, ITCOLD and Studio Pietrangeli, Italy
A. Possenti, University of Pisa, Italy
F. Angeletti and F. Ferranti, Studio Pietrangeli, Italy

The paper presents the results of a study on the behaviour of a small islanded grid, supplied only by hydro units, following generation and load disturbances. Based on a simplified model of the hydraulic components, the generation units and the electrical network, a system simulator provides values for frequency, loads and surge tank levels during the transients following such disturbances. Suitable power and frequency controllers for the generating units were synthesized, on the basis of geometrical and hydraulic characteristics of the penstock, the opening and closing time of the turbine valve actuator, and the starting time of the network, and then introduced in the model.The results show that, with a correct tuning of the turbine controllers, the grid can withstand large generation and load disturbances, with limited and quickly dampened oscillations both of frequency and surge tank level.

The case study described here relates to an islanded power network (see Fig. 1), supplied only by hydroelectric units with the following characteristics:

- Overall rotating power, 2500 MW.
- Two 1000 MW hydroelectric equivalent units, Plant A and Plant B, each supplied by the same reservoir but by separate tunnels/surge tanks/penstocks. Both A and B are equipped with five 200 MW Francis turbines. The hydraulic system is shown in Fig. 2.
- One 1500 MW equivalent unit, Plant C, equipped with a number of Francis and Pelton units and no surge tank.

1.1 Power network parameters

The following values have been assumed in the grid analyses, at least as a first approximation.

- load/frequency characteristic (load regulating energy), 50 per cent in the controller synthesis and 100 per cent in the transient simulations;
- starting time of the network, 10 s;
- normal range of frequency variation Δf, ± 2 per cent (± 1 Hz);

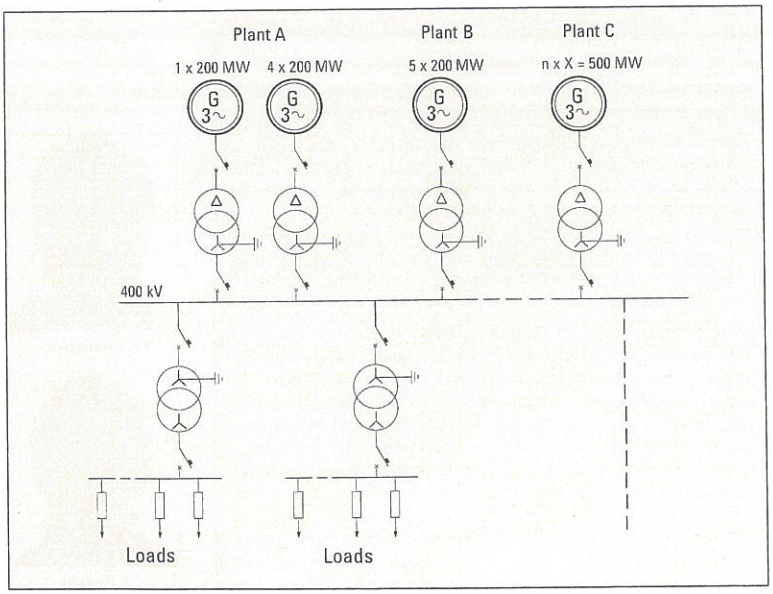

Fig. 1. Schematic diagram of the electrical grid.

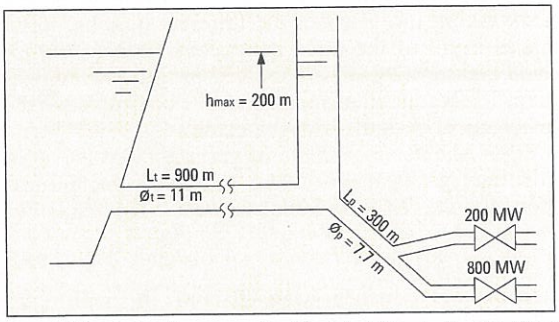

Fig. 2. The hydraulic system for Plant A. (It is similar for Plant B, but with one 1000 MW unit).

- first load-shedding level at 48.6 Hz with a 0.1 s delay;
- second load-shedding level at 48 Hz with 0.1 s delay; and,
- trip of the generating units at 47.5 Hz, with a 30 s delay.

1.2 Geometrical and hydraulic characteristics of Plants A and B

The main parameters are shown in Table 1.

The diameter of the surge tank was chosen by the plant designers on the basis of the total load rejection transient, followed by reloading at the most unfavourable time for the surge tank level. In other words, it has been verified that the surge tank size is adequate to prevent water overflowing during the upward surge, and the uncovering of the tunnel ceiling during the downward surge.

Table 1: Geometrical and hydraulic data for Plants A and B

Head, h (m)	120 (min) to 200 (max)
Flow rate, q (kg/s)	3.7×10^5 (min)to 4.7×10^5 (max)
Tunnel length, L_t (m)	900
Tunnel diameter, ϕ_t (m)	11
Tunnel cross-sectional area, A_t (m^2)	95
Surge tank diameter, ϕ_s (m)	20
Surge tank cross-sectional area, A_s (m^2)	314
Penstock length, L_p (m)	300
Penstock diameter, ϕ_p (m)	7.7
Penstock cross-sectional area, A_p (m^2)	46.6

The surge tank is also equipped with a throttle (with a diameter of 5 m) at the bottom, the slight dampening effect of which has been taken into account in the simulation model.

The other parameters used in the transfer functions, of interest for the study of the behaviour of the units during the transients, are listed in Table 2.

2. Linearization of hydraulic parameters

The values of parameters in Table 2 have been calculated based on the following simplified assumption:

- inelastic water column theory for incompressible flow;
- model transfer functions based on concentrated impedance method; and,
- linear behaviour of the system for small power system perturbations.

These assumptions are consistent with the aim of the study, that is, the analysis of frequency, load and shaft level transients, and not a detailed analysis of hydrodynamic and electromechanical phenomena in the generating units during grid disturbances.

For this purpose, the above assumptions are conservative.

The following expressions have been used:

- flow to the turbine through a valve of A opening:

$$q = A\sqrt{2gh}$$

- hydraulic/mechanical/electrical power:

$$P \equiv q \cdot h$$

- per unit variations of flow and power versus valve opening:

$$\frac{\delta q}{q} = \frac{\delta A}{A} + \frac{1}{2}\frac{\delta h}{h}$$

$$\frac{\delta P}{P} = \frac{\delta q}{q} + \frac{\delta h}{h} = \frac{\delta A}{A} + \frac{3}{2}\frac{\delta h}{h}$$

- linearized hydraulic resistance:
  being the head loss at flow q, so that:

$$\Delta = {}_{\max}\left(\frac{q}{q_{\max}}\right)^2$$

the linearized resistance

$$\frac{\delta\Delta}{\delta q} \quad \text{is} \quad R = \frac{2\Delta}{q}$$

Similarly, the equivalent resistance of the turbine valve, defined as

$$R = \frac{\delta h_v}{\delta q}$$

is equal to:

$$\frac{2h_v}{q}$$

where h_v is the water head upstream from the valve.

The same relationship can also be obtained by differentiating the relationship:

$$q = A\sqrt{2gh}$$

- hydraulic inductance of a conduit with length L and cross sectional area A, is defined by the relationships:

$$\Delta_t = -\Gamma\frac{dq}{dt}$$

$$A\Delta p = \frac{d}{dt}(mv)$$

and hence

$$\Gamma = \frac{L}{\rho g A}$$

m being the mass in the conduit and v its velocity.

- hydraulic capacitance: the hydraulic capacitance of the surge tank is easily obtained from the relationship:

$$q_s = \rho A_s \frac{dh_v}{dt}$$

q_s being the flow going into the surge tank.

Hence the capacitance is:

$$C = \rho A_s$$

3. Modelling the penstock-turbine valve complex

From the equation:

$$-\delta h_v = R_p \delta q + \Gamma_p \frac{d}{dt}\delta q \qquad \text{... (1)}$$

which after L-transformation becomes:

$$-\delta h_v = \left(R_p + s\Gamma_p\right)\delta q \qquad \text{... (1b)}$$

and form the relationships:

$$\frac{\delta q}{q} = \frac{\delta A}{A} + \frac{1}{2}\frac{\delta h}{h} \qquad \text{... (2)}$$

$$\frac{\delta P}{P} = \frac{\delta q}{q} + \frac{\delta h}{h} \qquad \text{... (3)}$$

$$R = \frac{2h}{q}$$

being $R >> R_p$ ... (4)

one can obtain the following block diagram:

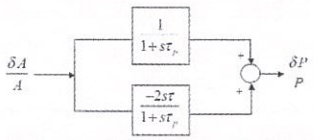

The transfer function between valve opening and power variation is thus:

$$\frac{\delta P}{P} \Big/ \frac{\delta A}{A} = \frac{1-2s\tau_p}{1+s\tau_p}$$

where $\tau_p = \Gamma_p/R$.

The above transfer function having a positive zero, it is of the 'non minimum phase' type.

The above model is the one used for the synthesis of the turbine controller.

Table 2: Linearized hydraulic parameters

Parameters	h_{max}	h_{min}
Head, h (m)	200	120
Linearized hydraulic resistance of the tunnel, R_t (ms/kg)	6×10^{-6}	4.7×10^{-6}
Linearized turbine characteristic, R (m/kg)	8×10^{-4}	6.5×10^{-4}
Linearized hydraulic resistance of the penstock, R_p (m/kg)	10^{-5}	8×10^{-6}
Hydraulic inductance of the tunnel, Γ_t (ms²/kg)	9×10^{-4}	9×10^{-4}
Hydraulic inductance of the penstock, Γ_p (ms²/kg)	6×10^{-4}	6×10^{-4}
Time constraint of τ_p penstock/turbine valve, τ_p (s)	0.75	1.1

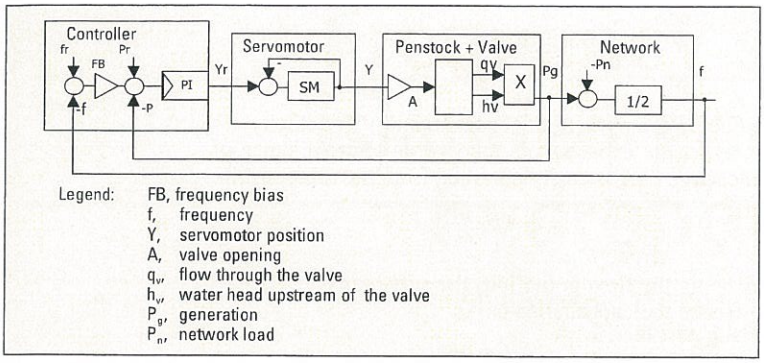

Fig. 3. Block diagram of the power/frequency control system.

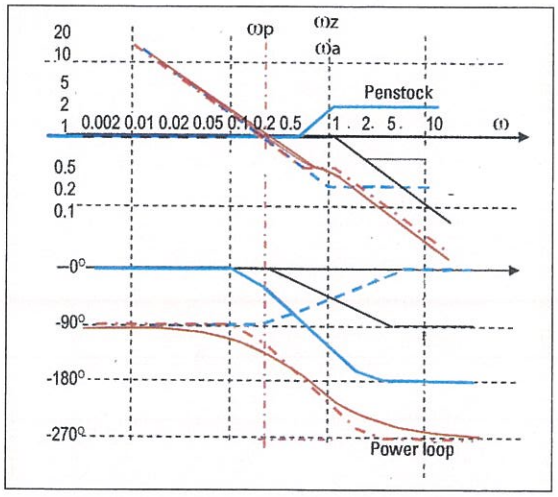

Fig. 4. Bode diagram of the power loop.

The transfer functions, also including the tunnel and the surge tank, are reported in the Appendix.

With the data listed in Table 1, namely: penstock length, 300 m; penstock cross-sectional area, 46 m^2; water head h, ranging from 200 to 120 m; and, flow rate q ranging from 4.7 to 3.7 × 10^5 kg/s: τ_p varies from 0.75 to 0.9 s respectively for h_{max} and h_{min}.

A value of τ_p =1 s has been always cautiously assumed in the following.

4. Synthesis of the power/frequency controller

Plants A and B (5 × 200 MW each) are controlled based on a scheme usually adopted for large units, that is, with two feedback control loops: the inner one is the power loop, and the outer one is the frequency loop. The power loop allows for direct control of the generation and, at the same time, reduces the variations in gain and the non-linearities of the turbine valve.

The reference value is set by the operator, or by the load dispatching centre, while the outer loop takes care of the frequency variations and changes the power set-point accordingly, with a high gain (frequency bias).

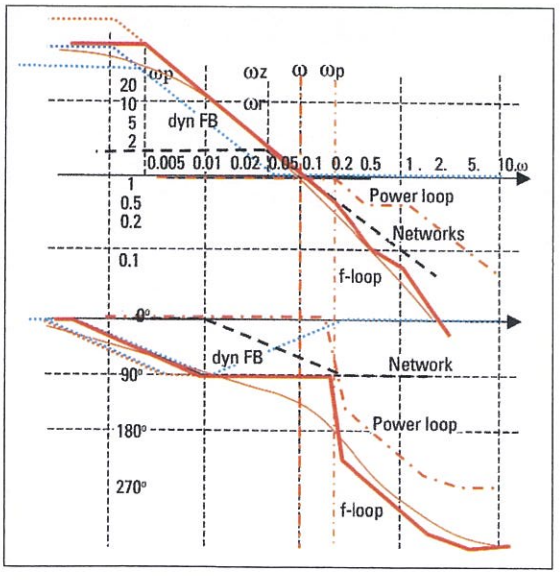

Fig. 5. Bode diagram of the frequency/ power loop.

4.1 Power loop (see Figs. 3 and 4)

The inner loop, including a PI controller, the valve servomotor and the penstock+turbine valve, shows a phase diagram mainly influenced by the non minimum phase function of the penstock-valve complex.

The linear approximation of the valve actuator (non-linear because of the speed limitation of 10 per cent/s of the servomotor) has a pole at τ= 1 s

As seen in Section 3, the penstock-valve-turbine has a 'non-minimum phase' pair pole-zero (pole at τ_p=1 s, zero at 2τ_p=2 s): this gives gain 1 and asymptotic 0° phase at $\omega < 0.1$, and gain 2 and -180° phase at $\omega > 5$ rad/s

Setting the zero of the controller at the pole of the servomotor ($\omega_z = \omega_p$ = 1 rad/s), the open loop phase diagram is similar to the one of the penstock, only shifted by a further phase lag of 90°. The cut-off frequency ω_p can be put at 0.2 rad/s, where the phase margin is 45° and gain is 1. The controller integral time T_i is so 1 / ω_p= 5 s and gain G_p is 0.2.

The power closed loop will then show a quick and stable response, with critical dampening and adequate phase and gain margins.

The phase lag of 270° at $\omega > 2.5$ rad/s is due for 180° to the non-minimum phase zero of the penstock + valve complex. Its behaviour is then similar to a pole T_p = 5 s, except at the beginning of the transient when its response is of opposite sign (see Fig. 5).

4.2 Frequency loop (Fig. 5)

The outer frequency loop includes the power network and the above closed power loop.

The power network has been assigned a starting time T=10 s and a relative load regulating energy equal to 0.5.

The transfer function load-to-frequency then becomes:

$$\frac{\Delta P_u}{P_{in}} = \frac{1}{1/2+10s}\frac{\Delta f}{f}$$

which gives permanent gain 2 and asymptotic 0° phase at $\omega < 0.01$, and 0 gain and -90° phase at $\omega >$ 0.25 rad/s.

To obtain a quick and stable control, the cut-off pulsation ω is set at 0.1 rad/s. The frequency bias zero is set at the network pole, 0.05 rad/s, with gain equal to 1. The frequency bias pole ω_p is set in such a way not to change the phase margin of the f-loop. Therefore, with ω_p = 0.002 rad/s the permanent droop is 4 per cent (gain = 25) or, with ω_p = 0.001 rad/s, the permanent droop is 2 per cent (gain = 50).

With the above parameters, the frequency loop shows a quick response, with critical dampening and response time $\tau = 1/\omega$ = 10 s, which is an adequate value for the network frequency control.

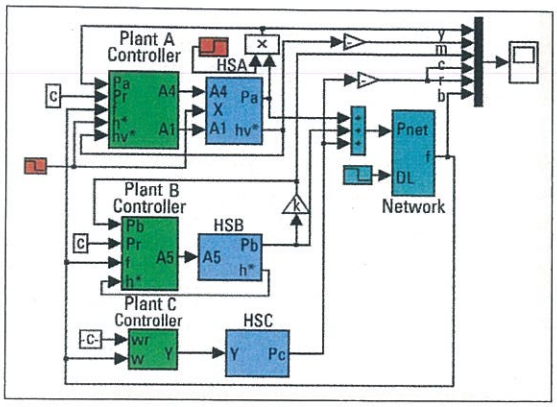

Fig. 6. Simulator of the grid (three equivalent groups of units for plants A, B and C).

5. Synthesis of the speed controller

In the case study, Plant C has only been equipped with a speed controller, as is customary for small power units.

The permanent droop is set at 2 per cent, which means a proportional gain of 50.

Using the traditional criteria for controller design (not reported here for the sake of brevity), a quick and stable response of the speed loop is obtained with a PI controller with proportional gain G_p=50 and Integral time Ti= 10 s.

6. Simulation of some transients

Using the MATLAB/SIMULINK programme, a number of particularly severe transients have been simulated under the following assumptions.

Plants A and B are equipped with the power/frequency controller described in the previous paragraph.

Plant C is equipped only with the frequency controller, as mentioned previously.

Some SIMULINK block diagrams are shown in Figs. 6, 7 and 8. The tunnel, surge tank and penstock are introduced in the model with the unsteady flow equations for incompressible fluids.

The power controller of Fig. 8 includes, besides the 'frequency bias', the option for a 'level bias' signal which produces a dampening effect.

As the 'frequency bias' signal changes the basic power demand to control the grid frequency (by the outer frequency loop), so the 'level bias' signal changes the power demand proportionally to the level

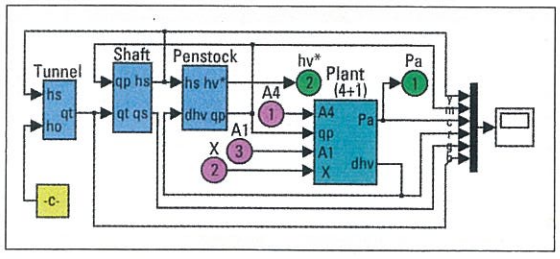

Fig. 7. Model of the hydraulic system.

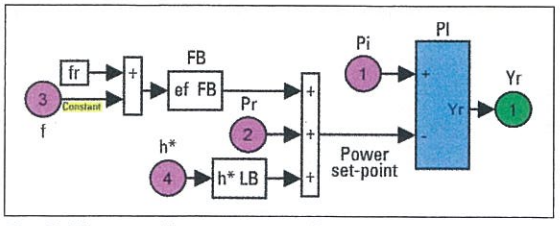

Fig. 8. The power/frequency controller.

variations in the surge tank (and to the head upstream of the turbine valve), so that the power controller is forced to 'accept', or even enhance, the power variations caused by the water head variations.

Plant A, supplied by the hydraulic system comprising the tunnel, surge tank and penstock, has been split into two equivalent sub-groups, each including its own valve and generator, one of 800 MW and the other of 200 MW capacity.

In this way, it is possible to simulate accurately the trip of this last unit (with the correct closing time of the valve) and the response of the four units remaining in operation under their power controller.

The cases examined all include a double disturbance, one in generation, and the other one in load, the latter delayed by about 1000 s. The simulation does not take into account the intervention of the load shedding relays during the frequency drop, the effect of which would benefit stability.

6.1 Case 1

All units in operation at about 80 per cent of rated load, 2000 MW is the network overall load.

- Maximum reservoir level, w.h. 200 m.
- At time 0, the tripping of one unit of Plant A – 160 MW generation loss, 20 per cent of the plant's capacity, and 8 per cent of network load.
- After about 1000 s, loss of an equal network load (160 MW).

Fig. 9. Case 1, (h_{max}).

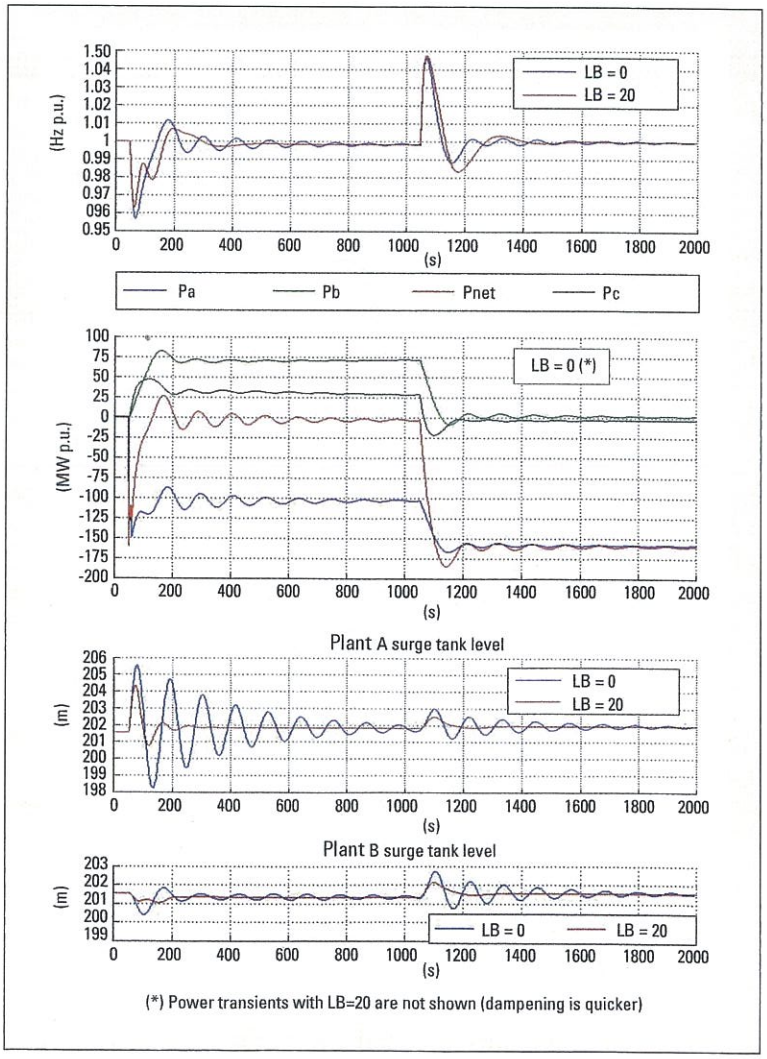

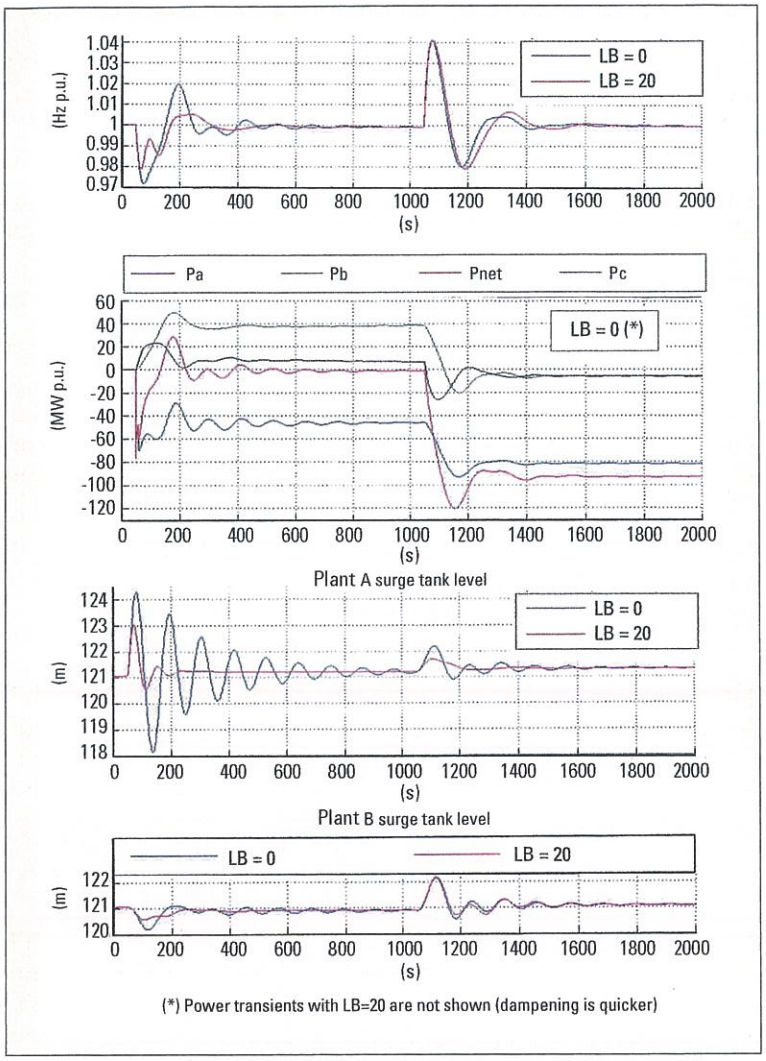

Fig. 10. Case 2 (h_{min}).

With 0 'level bias', the values of frequency, loads, and shaft levels during the transient are shown in Fig. 9: the transient (more severe for Plant A) is dampening within a few minutes.

Frequency variations are within ± 2 Hz, and shaft level variations within ± 4 m.

With 'level bias' gain = 20, the dampening of the transient is much quicker, and both level and frequency variations are smaller.

6.2 Case 2

- Reservoir level at minimum, w.h. 120 m.
- Plants A and B generating 380 MW each, that is ~ 40 per cent of rated power (80 per cent of maximum possible generation at minimum water head). Plant C at 80 per cent of rated load, that is 400 MW.
- Overall grid load, 1160 MW.

At time 0, the tripping of one unit at Plant A (76 MW), and after ~ 1000 s, loss of 90 MW of grid load.

As can be seen in Fig. 10, with 0 'level bias' the frequency variations are smaller compared with the previous case (-1.4 Hz to + 2 Hz), because the disturbance is smaller (6.5 per cent rather than 8 per cent of current load).

Again, results are better if the 'level bias' gain is 20.

6.3 Case 3

The following limit situation was also tested:

- Only Plant A in operation at 80 per cent rated power. Overall network load, 800 MW.
- At time 0, trip of one unit (generation loss 160 MW, 20 per cent current load) and after 1000 s loss of an equal network load.

Frequency variations are of course larger (-8 per cent, +5 per cent), while the surge tank level oscillations are ± 4 m as a maximum. Both are quickly dampened. The stability is also assured in this situation, which in any case is a situation which grid managers will certainly try to avoid. As a result of the correct intervention of the load shedding relays, a blackout could be prevented.

7. Conclusions

This study shows that, with an appropriate tuning of turbine controllers, an islanded power grid, supplied only by hydroelectric units, can withstand large generation and load disturbances while frequency oscillations are maintained within acceptable limits, and power transients are quickly dampened.

The level swings in the surge tanks are also very limited and quickly dampened, even if the cross sectional area of the surge tanks is smaller than the Thoma value.

This is particularly true if a 'level bias' is introduced in the turbine power controller.

In fact, with the assumptions made for the hydraulic system, the generation units and the power network, the cross-sectional area of the surge tanks (chosen according to the criteria recalled in section 1) turns out to be to a large extent irrelevant for the frequency stability of grid and the hydraulic stability of the surge tanks themselves.

Appendix

1.Thoma's hypothesis

This is based on a hydraulic scheme without a penstock, including: a reservoir, tunnel, surge tank and turbine valve (see Fig. 11).

The transfer function (for small perturbations) between the valve flow and the shaft level is:

$$\frac{\delta h}{h}\Big/\frac{\delta q}{q} = -\frac{2}{R}\frac{Z_t}{(1+sqA_sZ_t)}$$

where:

$$Z_t = R_t + s\Gamma_t$$

is the tunnel impedance, and:

$$R = \frac{2h}{q}$$

is the linearized resistance of the control valve.

The 2nd order function has a pulsation:

$$\omega = \frac{1}{\sqrt{\rho A_t \Gamma_t}}$$

and a dampening factor:

$$\varsigma = \frac{1}{2}\omega(\tau_t + \rho R_t A_s)$$

where:

$$\tau_t = \frac{\Gamma_t}{R}$$

In our case (see Tables 1 and 2):

$\omega = 0.06$ rad/s

$\tau_t = 1.1$ s

Thoma's condition:

$$\frac{\delta P}{P}=\frac{\delta q}{q}+\frac{\delta h}{h}=0$$

can be translated into the following block diagram:

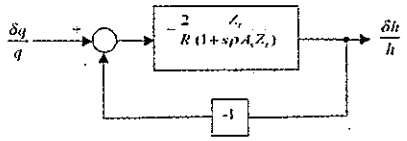

The closed loop transfer function is:

$$\frac{\delta h}{h}=-2\frac{Z_t}{R+s(\rho A_s RR_t-2\Gamma_t)+s^2\rho RA_s\Gamma_t}\frac{\delta q}{q}$$

The stability condition requires that the s term in the denominator be ≥ 0, this means the shaft cross-sectional area will be:

$$\bar{A}_s \geq \frac{2\Gamma_t}{\rho RR_t}$$

In our case $\bar{A}_s$ (Thoma's area) would be about 370 m².

If, rather than applying the above algebraic feedback directly, we apply it through a time constant

$$\frac{1}{1+s\tau}$$

the critical area becomes smaller, in fact much smaller: this is what would occur in a real plant, where the power level is kept constant by a real controller through a chain of components consisting of valve servomotor with its speed limits, generating units with their inertia, controller with its transient droop and integral time.

For example, in our case, with τ = 10 s, the critical area will decrease from 370 to 220 m² (ϕ 16.7 m).

If a hydraulic system is considered which also includes the penstock, (Fig. 12) the relevant transfer functions will be as follows

$$\frac{\delta h_s}{h_s}=-2\frac{Z_s}{Z_t+Z+s\rho A_s Z_t}\frac{\delta A}{A}$$

where $Z = Z_p + R$ and Z_p is the penstock impedance.

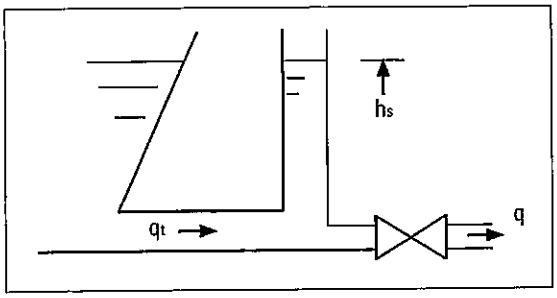

Fig. 11. Hydraulic system without penstock.

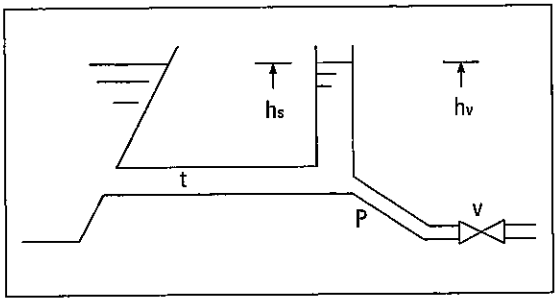

Fig. 12. Hydraulic system with penstock.

Notations

h_o	=	reservoir level (m)
h_s	=	water head at surge tank bottom (m)
h_v	=	water head at turbine valve (m)
q_t	=	tunnel flow (kg/s)
q_s	=	flow into shaft (kg/s)
q_p	=	penstock flow (kg/s)
q_v	=	valve flow (kg/s)
A	=	valve opening (p.u.)
Y	=	servomotor position, (p.u.)
P_g	=	generated power (MW)
P_n	=	network load (MW)
FB	=	frequency bias
LB	=	level bias
L_t	=	tunnel length (m)
A_s	=	surge tank cross sectional area (m²)
L_p	=	penstock length (m)
w.h.	=	water head (m)
ρ	=	water specific gravity (1000 kg/m³)

$$\frac{\delta h_s}{h_s}=-2\frac{Z_t+Z_p(1+s\rho A_s Z_t)}{Z_t+Z(1+s\rho A_s Z_t)}\frac{\delta A}{A}$$

Developing the function for a small step of $\frac{\delta A}{A}$, one can see that the shaft level oscillates more or less at the same frequency as it does without the penstock (ω = 0.06 rad/s in our case).

Here again one can impose the Thoma (or Thoma-Evangelisti) condition, which is:

$$\frac{\delta P}{P}=\frac{\delta A}{A}+\frac{3}{2}\frac{\delta h}{h}=0$$

to find the stable cross-sectional area of the shaft.

The above condition can be translated into the following block diagram

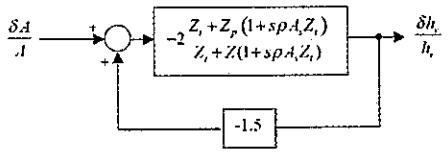

from which, as a first approximation, the critical area of the shaft will be:

$$\bar{A}_s=\frac{2\Gamma_t}{\rho RR_t}\left(1+\frac{\Gamma_p}{\Gamma_t}\right)$$

Here again one can see that, introducing the feedback with a time constant:

$$\frac{1}{1+s\tau}$$

the shaft cross-sectional area may be much smaller.

In our case, with τ = 10 s, the level oscillations in the surge tank will always be dampened, no matter how small the shaft area is.

From a qualitative point of view, this is what happens in a real plant where the power controller, aimed at maintaining the power at the set point value in a stable and smooth manner, "sees" the level disturbances through the whole chain of servomotor, network, and so on.

The simulations carried out with SIMULINK confirm the above results in the realistic cases examined.◊

Acknowledgement

The authors express their warm thanks to G. Ferrazza and C. Reynaud of Studio Pietrangeli for their collaboration in the developing phase of the study

Bibliography

Nicolet C. et al., "Transient phenomena etc.", IAHR/AIRH Congress, Stuttgart, Germany ; 2003.

Evangelisti, G., "Stabilità dei sistemi complessi etc." *L'Energia Elettrica,* Vol. 32; 1955.

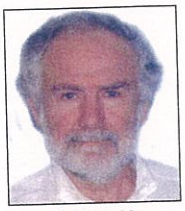

M. Cadeddu

A. Possenti

F. Ferranti

F. Angeletti

Massimo Cadeddu, former Director of the Hydroelectric Sector of Enel, and Past President of ItCOLD, has for many years served as a consultant to Studio Pietrangeli for the design and specifications of electromechanical equipment for hydroelectric projects.

Italian Committee on Large Dams, Via dei Crociferi 44, 00187 Rome, Italy.

Andrea Possenti, former Manager of the Automatic Control Systems Department at Enel's Power Production Division, is currently consultant to Pisa University and Studio Pietrangeli in the field of control system engineering.

University of Pisa, Lungarno Pacinotti, 56126 Pisa, Italy.

Federico Ferranti is a Civil Engineer. He graduated in 2005 from L'Aquila University, Italy. Since 2006 he has been working with Studio Pietrangeli, mainly in the field of hydraulic design of hydraulic structures for dams and hydropower projects. In 2009 he was awarded his PhD in Environmental and hydraulic engineering at the L'Aquila University of Pisa, Italy.

Fabio Angeletti is an Electrical Engineer. He graduated in 2008 from the University La Sapienza of Rome, Italy. He has been involved in design of electromechanical equipment for several hydropower plants with Studio Pietrangeli. He has also been teaching at Technical Institute of Terni Lorenzo Allievi, Italy.

Studio Pietrangeli SRL, Via Cicerone 28, 00193 Rome, Italy,